

Oil immersion Cooling of Lithium-Ion Battery Modules: Numerical Modeling and Flow Visualization

Safouene Ouenzerfi¹, Rodrigo Amorim Dias², Julien Plet², Riadh Bouabker¹, Souad Harmand¹

¹ LAMIH Université Polytechnique Hauts-de-France,
(corresponding author) safouene.ouenzerfi@uphf.fr

² MOTUL, Vaires sur Marne

Executive Summary

Battery thermal management systems (BTMS) are vital for ensuring the optimal performance and safety of high-performance electric vehicles (EVs), where efficient heat dissipation and temperature homogenization within individual cells and packs are critical. Several BTMS solutions are available, ranging from active air cooling to indirect liquid-based methods like plate cooling. While liquid-based systems are typically more effective in heat removal than air-cooled systems due to their higher convective transfer coefficients and specific heat capacities, they often come with increased complexity and weight. Immersion cooling is an emerging alternative, where the battery cells are directly submerged in an electrically insulating fluid. This method offers a significant advantage in heat transfer performance, as the direct contact between the cells and the immersion fluid facilitates more efficient thermal management. Additionally, the fluid can serve as a thermal barrier if it has low flammability, adding an element of safety.

When evaluating immersion cooling solutions, the fluid properties—such as viscosity, thermal conductivity, density, heat capacity, flammability, and material compatibility—play a crucial role. One key challenge is the trade-off between viscosity and thermal conductivity; improving the thermal conductivity of an oil often leads to an increase in its viscosity, which can impact flow and heat transfer performance. In this study, we experimentally compare three different fluid formulations, each with varying levels of viscosity and thermal conductivity, to better understand their performance in immersion cooling systems.

A numerical study was conducted using Fluent and Discovery CFD platforms to assess the performance of the immersion cooling technique for a 15-cell module. We compared three industrial fluids, each with different characteristics in terms of thermal conductivity and viscosity. These numerical simulations allowed us to evaluate the impact of these properties on cooling efficiency and identify the most effective fluids for this specific application.

The comparison shows the depending on the flow rate. Additionally, we developed an experimental method to validate the numerical simulation approach. This approach allows for a better understanding of how fluid behavior influences the cooling performance across varying conditions. By combining numerical simulations and experimental observations, we can further refine the selection of the most suitable fluids for immersion cooling systems based on their dynamic performance under different operational scenarios.

1 Introduction

Immersion cooling has become an increasingly popular technology in recent years, particularly for electronic devices and the electric vehicle industry [1-2]. In this approach, the battery is fully immersed in a dielectric fluid (non-electrically conductive), establishing direct contact between the fluid and the battery cells. Common dielectric fluids used in immersion cooling include hydrocarbons, silicone oils, and fluorocarbons.

One of the main advantages of immersion cooling is its ability to provide excellent temperature uniformity across the entire battery pack and individual cells. Since all surfaces of the battery are in contact with the liquid, heat transfer is more efficient and homogeneous. This direct contact also reduces the thermal resistance typically encountered in indirect cooling systems [3]. Furthermore, immersion cooling simplifies the overall system design and reduces its complexity [4]. An additional benefit is the enhanced safety of immersion cooling systems, as some dielectric fluids are flame-retardant or fireproof, reducing the risk of thermal runaway in lithium-ion battery (LIB) packs.

Immersion cooling systems can vary based on the level of submersion, the flow pattern, and the operational properties of the fluid. Much of the recent research on immersion cooling has focused on the performance of individual cells and battery packs. For instance, Nelson et al. [5] conducted a thermal analysis comparing direct silicone oil cooling with air cooling in a 48-cell system. Their findings showed that direct silicone oil cooling resulted in a temperature increase of only 2.5°C, whereas air cooling led to a temperature rise of 5.3°C under the same charging conditions. Similar results have been reported by Karimi et al. [6-7], confirming the superior thermal performance of silicone oil cooling compared to air cooling.

The goal of this project is to investigate and evaluate the performance of immersion cooling technology when applied to a cylindrical battery cell module, with the aim of optimizing cooling efficiency and enhancing overall system performance. This is why we are numerically studying the performance of this cooling technique using three fluids with different characteristics. This approach allows us to analyze the impact of each fluid's thermophysical properties, such as viscosity, thermal conductivity, and heat capacity, on the overall cooling efficiency. By comparing the results for each fluid, we can determine which one provides the best thermal performance in the context of a 15-cell module and optimize the immersion cooling system accordingly.

2 Numerical simulations

2.1 Modeling methodology

ANSYS is a widely recognized software used for analyzing various engineering projects and conducting multiphysics simulations. Numerous researchers have utilized ANSYS in their studies [7–10]. In this work, we employed Ansys Fluent, initially version 15 (and subsequently version 2024) and then we employ Discoverey 2023, to simulate immersion cooling with fluid circulation for a Li-ion battery module. The sub-steps of the modeling process are detailed below.

2.1.1 Geometry

The reference geometry was designed using the SolidWorks CAD tool. It represents a section of a battery module composed of 15 cylindrical cells, based on commercial examples with a diameter of 21 mm and a height of 70 mm (see Figure 1). These cells are mounted in a support structure with dimensions of 100

mm \times 120 mm \times 150 mm and a thickness of 2 mm. The entire system is immersed in a fluid domain, with circular inlets and outlets (diameter: 10 mm) on either side for fluid entry and exit. This study investigates the modularity of the system, particularly the effect of inlet/outlet configurations, by exploring various positions for fluid entry and exit.

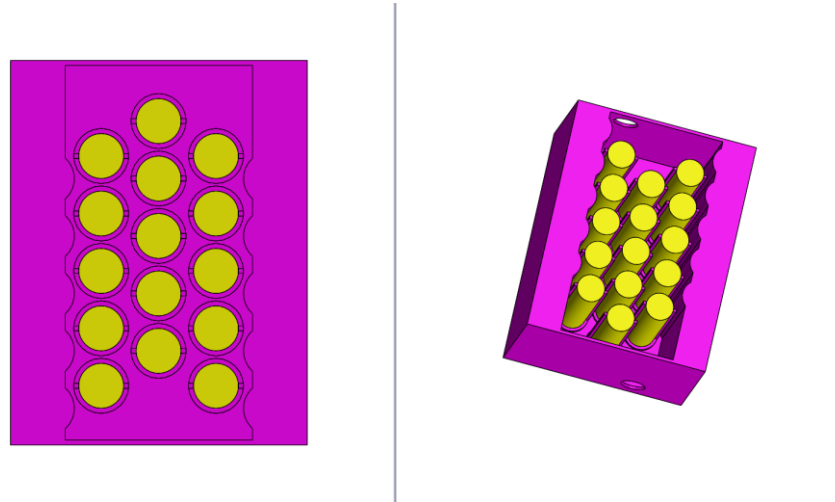


Figure 1: Geometry module design

2.1.2 Meshing

The mesh was automatically generated in ANSYS to achieve a target wall y^+ value around 30. A hybrid mesh dominated by hexahedral elements was used. To properly capture the fluid–cell interactions, a non-conformal interface was implemented, which avoids the need for a highly refined mesh. Inflation layers were also included to accurately resolve boundary layers. On average, each simulation involved approximately 800,000 nodes (see Figure 2).

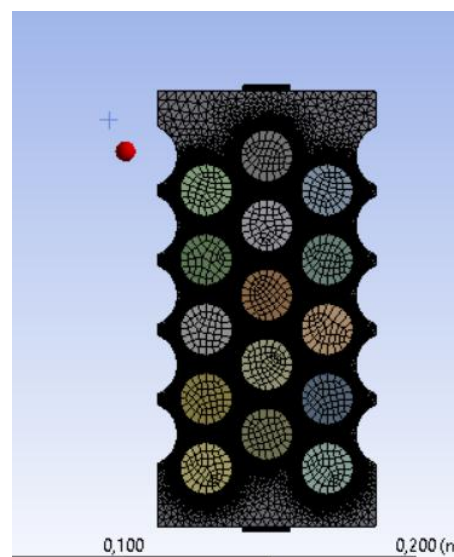


Figure 2: Meshing illustration

2.1.3 Numerical Models

As immersion cooling may involve laminar or turbulent flow, a turbulence model was required. For computational efficiency, a Reynolds-Averaged Navier-Stokes (RANS) approach was adopted. Within the k - ϵ turbulence model family, the Realizable k - ϵ model was chosen for its higher accuracy compared to the standard k - ϵ and greater flexibility than the RNG variant.

For heat transfer, the SIMPLEC algorithm was used to solve the energy equation, coupled with the velocity and pressure fields.

2.1.4 Materials

The working fluids were various MOTUL cooling oils, with air used as a reference case. The battery cells were modeled as aluminum, while the support structure was assigned material properties equivalent to PTFE or an insulating resin.

2.1.5 Boundary Conditions

A variable mass flow rate was applied at the inlet, along with a modifiable initial temperature, typically set to 20 °C. At the outlet, a standard atmospheric pressure condition was defined (see Figure 3). The cells act as heat sources, with a total Joule heating power defined in watts (W).

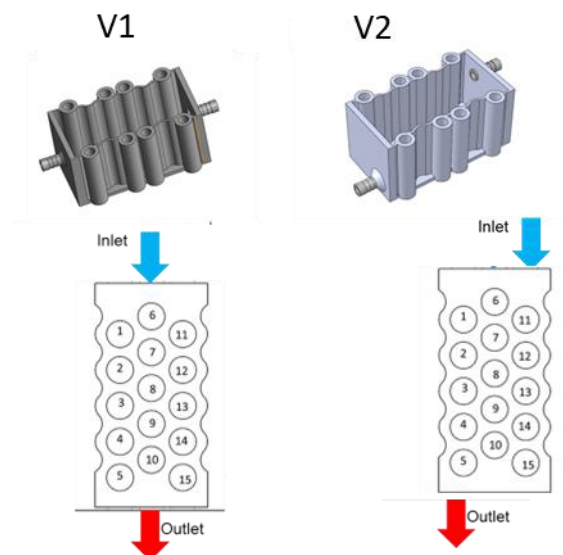


Figure 3: Inlet-Outlet localization for the configurations studied

2.2 Comparison with experimental tests

A test bench has been set up (Figure 6), featuring a resin support, heating elements, a pump, a temperature-controlled reservoir, and sensors to monitor cell temperature, flow rate, and pressure drops. Cell behavior is simulated using thermocouple-equipped heating cartridges, immersed in circulating dielectric oil. Electrical power is used to heat the cartridges. A volumetric pump ensures controlled fluid circulation, while oil inlet temperature is regulated in a separate reservoir using a Julabo-type immersion heater. Tests were also carried out with air by replacing the fluid inlet with an air supply.

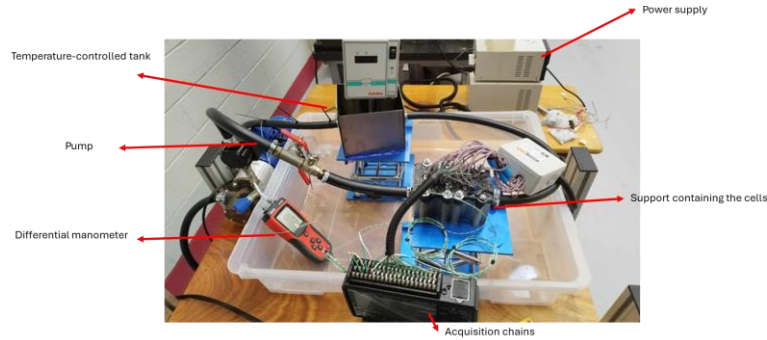


Figure 4: Experimental testbench for model validation

Figure 7 presents a comparison between the simulation values and the measured values for the 9 thermocouple positions at a power of 40W (1-C charge rate), showing good agreement between the simulation and the measurements.

We observe that the lowest temperatures are located near the inlet, while the highest temperatures are found near the outlet, as the air has carried the heat primarily towards this area. It is important to note that, at 40W, the temperatures exceed 60°C, which could pose a risk to the lifespan of the cells.

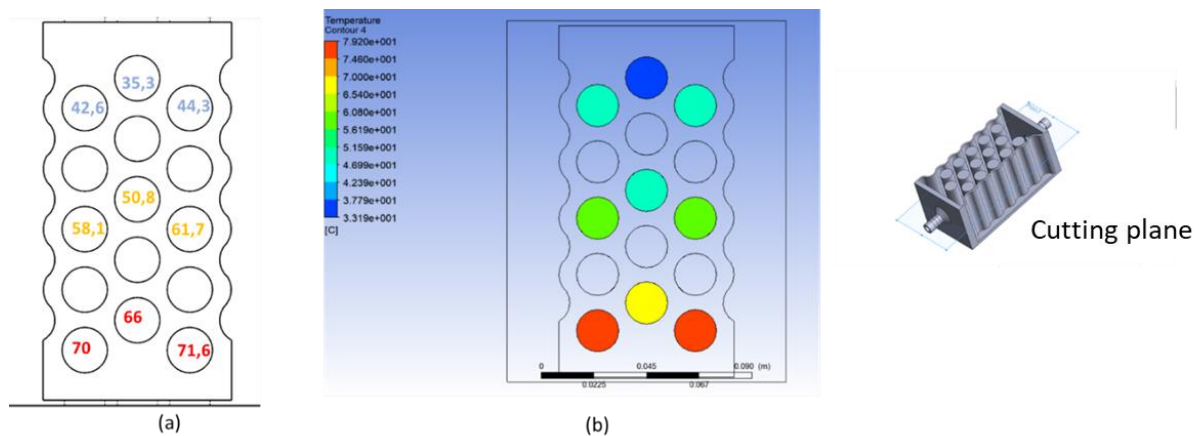


Figure 5: Cross-sectional comparison of the temperature distribution over 9 cells for a power of 40W and an air flow rate of 25l/min between a) experimental results and b) results from Fluent simulation.

2.3 Discovery and Fluent comparison (reference case: air as fluid)

Before conducting tests with oil, we first decided to study the test bench using air cooling, as it is a well-established cooling method in both the literature and in modeling. This approach will allow us to later compare these results with those obtained using oils.

We established reference simulations with air as the immersion fluid, using an inlet flow rate of 20 L/min (a common flow rate in our experimental setups) and an inlet temperature of 20°C. The simulations were carried out at several power levels.

For example, with a total power of 60W, the results provided insights into the temperature levels across all the cells as well as the velocity distribution on a cross-sectional plane. Figure 4 shows the temperature distribution on the cells using both the Fluent and Discovery methods. Figure 5 more quantitatively illustrates the error between the two simulations, which is approximately 2%.

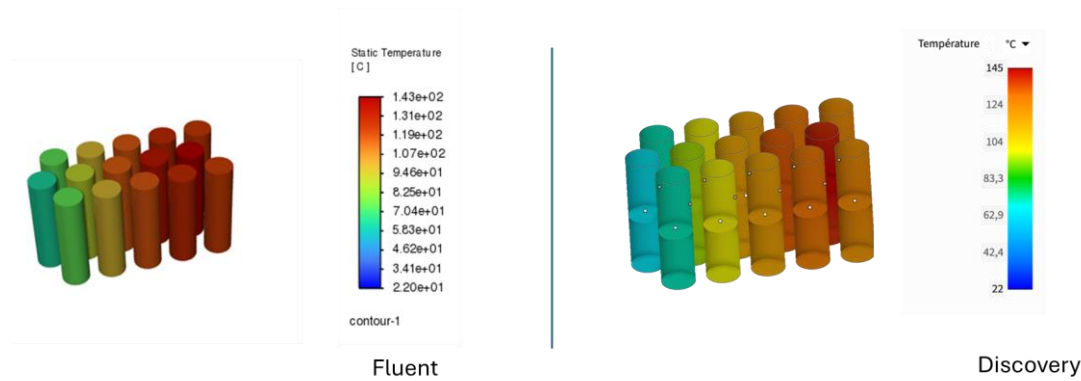


Figure 6: Temperature distribution on a cutting plane with Fluent and Discovery for 60W and 20l/min as inlet flow rate

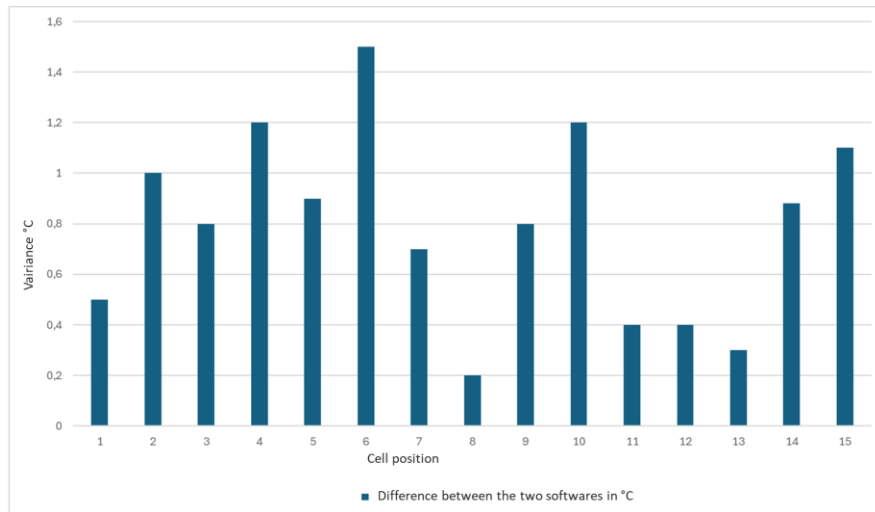


Figure 7: Difference in temperature values between Fluent and Discovery simulations

3 Fluids choice

As previously mentioned, 3 fluids developed by MOTUL will be the subject of the experimental study in the static immersion phase. The formulation of these oils is confidential, and their properties (thermal capacity, thermal conductivity and viscosity) have been measured using MOTUL's in-house resources (see annexed figures). The three oils are designated as follows

a) HV oil: This oil is characterized by high viscosity, hence the name High Viscosity (HV).

b) LV oil: Low viscosity, hence the name Low Viscosity (LV).

c) MV oil: This oil is characterized by a viscosity somewhere between the two (LV and HV), hence the name Medium Viscosity (MV).

The choice of this range of oils was based on their excellent dielectric properties (in MOTUL's experience). In addition to their insulating properties, fire safety is a prime consideration in the choice of dielectric fluids. The fluids studied have interesting flammability characteristics, influencing their suitability for different applications. A thorough understanding of these properties enables the most appropriate fluid to be selected according to the specific requirements of each application.

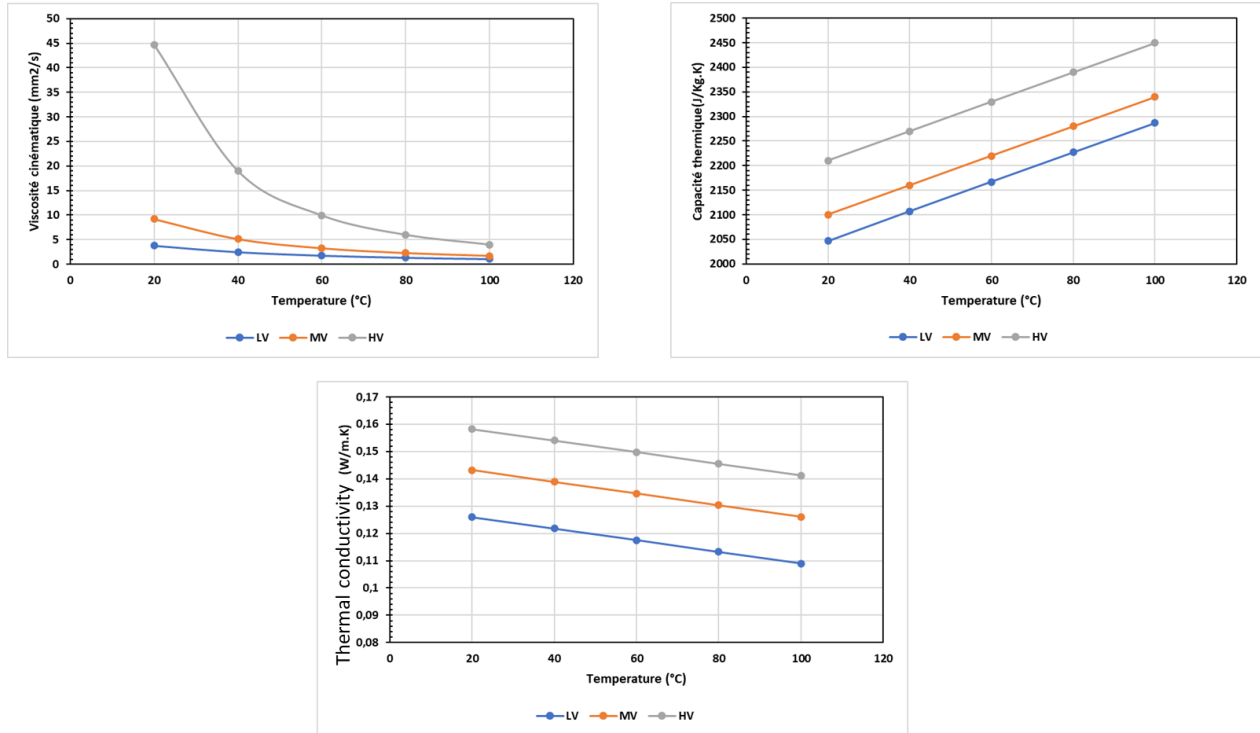


Figure 8: Thermophysical proprieties for the studied dielectric fluids

4 Key results simulations

In this section, we present a selection of key simulation results performed on Discovery. The first part focuses on studying the effect of flow rate on temperature distribution. The second part explores the influence of flow rate on fluid dynamics, particularly the transition to turbulence under certain operating conditions. The final illustration presents a comparison of the three fluids in terms of flow behavior for a specific configuration

The graph on figure 9 shows steady-state simulation results for a charge rate of 3C (100 W) using the LV fluid, for two flow rates: 0.5 and 2 L/min. The first observation is a temperature reduction of approximately 17°C of T_{max} when increasing the flow rate from 0.5 to 2 L/min. Secondly, the maximum temperature difference within the module at 2 L/min is around 10°C, which remains relatively high. It can also be concluded that, for this fluid, the maximum temperature exceeds 50°C at 0.5 L/min, which could pose a risk to battery safety. Additionally, it is observed that hot spots tend to appear near the outlet, although their exact location also depends on the flow rate.

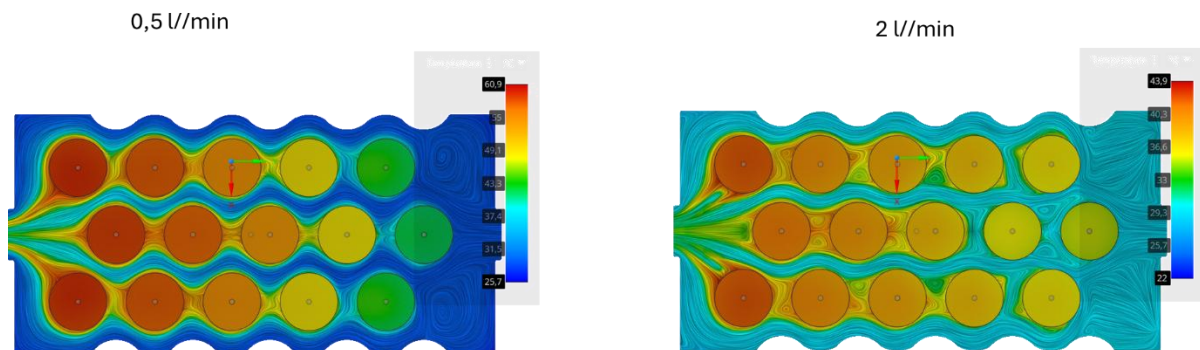


Figure 9: Flowrate effect on temperature distribution for LV fluid with 3C charge rate

The figure presents a dynamic fluid simulation considering the HV fluid, for a total power of 100W, at different flow rates. The results show that at 0.5 L/min, only a small vortex is observed near the inlet. However, at 3.5 L/min, the turbulence cells appear to be more widespread throughout the system. The appearance of generalized vortex cells from 3.5 L/min may be attributed to a transition to turbulent flow. We calculated the Prandtl and Reynolds numbers, as shown in the table. Based on these results, we assume that the flow becomes turbulent around a Reynolds number of 1000 in this configuration.

This relatively low critical Reynolds number is explained by the specific properties of the oil used, particularly its nature and viscosity (see table 1).

Table 1 : Reynolds and Prandtl number function of flowrate for HV fluid

Flowrate (l/min)	Prandtl number	Reynolds number
0,5	180,72	229,49
1	196,42	420,08
1,5	213,92	575,56
2	233,17	700,36
2,5	254,17	798,95
3	276,86	875,55
3,5	288,84	976,55

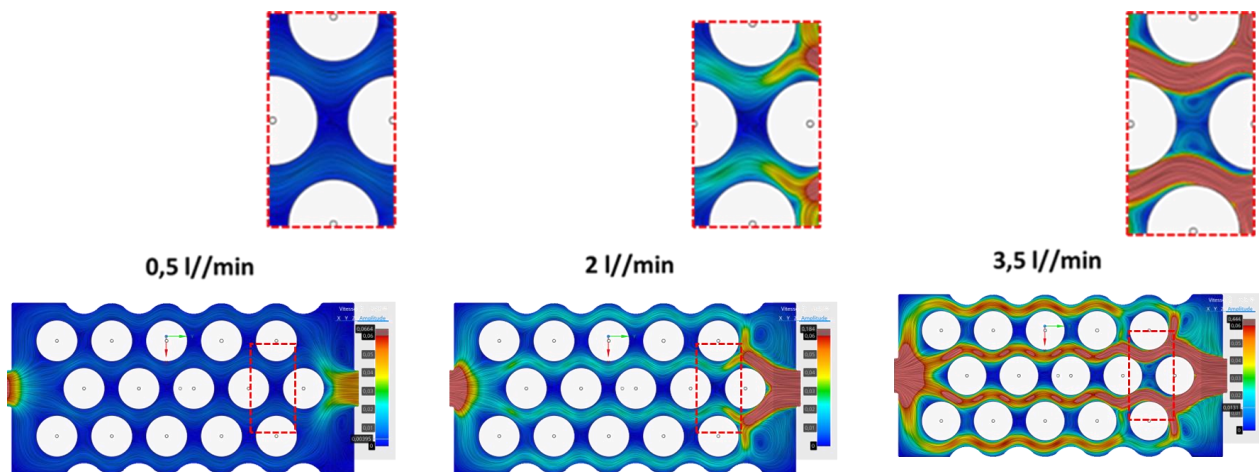


Figure 10: the results of the streamline distribution from the Discovery simulations on the central plane for different flow rates ($P_{tot} = 100W / 3C$, $T_{in} = 29^{\circ}C$, HV fluid, and configuration V1)

In the figure 11, we compared the flow behavior of the three fluids under the same conditions: 3C–100 W, $T_{in} = 29^{\circ}C$, flowrate=0,5 l/min using configuration V2. It was observed that the HV fluid exhibits a significantly different flow pattern compared to the other two fluids. Specifically, under the established flow regime with HV oil, the velocity streamlines (see Figure 11) tend to bypass certain

cells, following a diagonal trajectory instead. Due to its high viscosity, the HV fluid flows more slowly, allowing some streamlines to reach distant cells such as cells 6 and 11.

By analyzing the simulation cross-sections shown in Figure 80, the HV fluid follows a distinct circulation pattern from its first interaction with cell 1. Higher local viscosity leads to lower velocities around the cylinders and consequently results in a thicker boundary layer compared to the MV and LV fluids.

At such velocities, the HV fluid is unable to pass through the narrow gap between cells 1 and 6, instead following a preferential path toward cell 11. This phenomenon does not occur with MV and LV fluids, which, due to their lower viscosities, develop thinner boundary layers. This facilitates flow through the narrow region and allows more effective cooling of the affected cells.

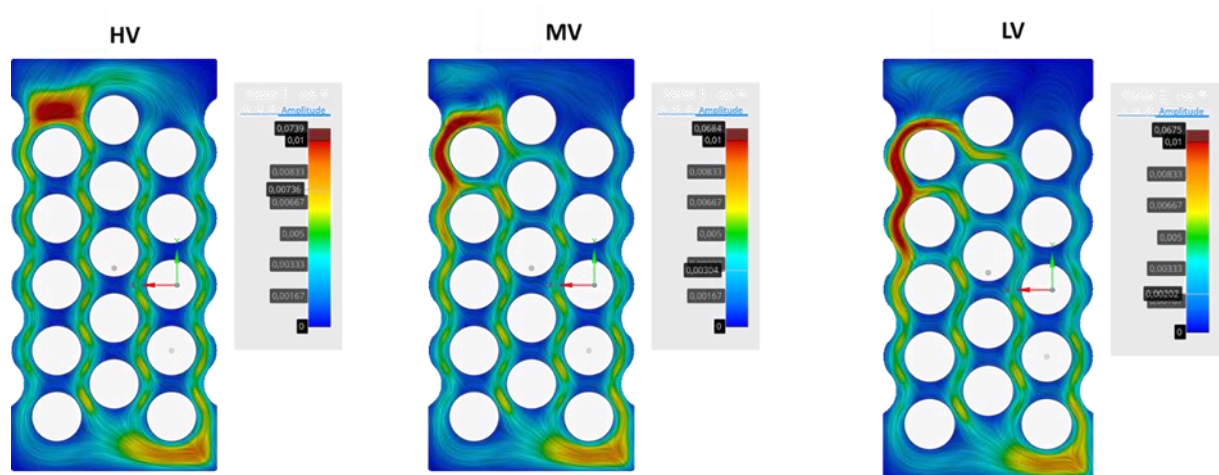


Figure 11 : Streamlines comparison between the three fluids for 3C, $T_{in}=29^{\circ}\text{C}$ 0,5 L/min and V2 configuration

5 Visualization process

We have set up an experimental bench that allows us to track the fluid flow from above. To do this, we 3D-printed a resin support that includes the shape of the cells. Using dye, we feed the fluid into the system and track its flow with a high-speed microscope camera. This setup enables us to visually monitor the flow dynamics and gain valuable insights into how the fluid behaves within the cooling system. This test setup will need to be further refined to enable a more detailed analysis of the flow behavior. However, at this stage, it already confirms the general flow direction (figure 12).



Figure 12: Visualization of the direction flow using colored tracer

Acknowledgments

This work has been carried out within the framework of a collaboration supported by ANRT (Association Nationale de la Recherche et de la Technologie) through the CIFRE program. The research benefits from the financial support of ANRT, as well as the technical expertise and resources provided by MOTUL. Their contributions have been essential in advancing the study of immersion cooling systems for battery modules.

References

- [1] Y. Deng, C. Feng, J. E. H. Zhu, J. Chen, M. Wen, H. Yin. (2018). Effects of different coolants and cooling strategies on the cooling performance of the power lithium-ion battery system: A review. *Applied Thermal Engineering*, 142, 10–29.
- [2] M. Al-Zareer, I. Dincer, M.A. Rosen. (2017). Novel thermal management system using boiling cooling for high-powered lithium-ion battery packs for hybrid electric vehicles. *Journal of Power Sources*, 363, 291–303.
- [3] Sahoo, P. (2021). A Review on Thermal Management in Electric Vehicle Battery System by Liquid Cooling. SAE Conference.
- [4] Y. Huo, Z. Rao. (2015). The numerical investigation of nanofluid-based cylinder battery thermal management using lattice Boltzmann method. *International Journal of Heat and Mass Transfer*, 91, 374–384.
- [5] P. Nelson, D. Dees, K. Amine, G. Henriksen. (2002). Modeling thermal management of lithium-ion PNGV batteries. *Journal of Power Sources*, 349–356.
- [6] G. Karimi, X. Li. (2013). Thermal management of lithium-ion batteries for electric vehicles. *International Journal of Energy Research*, 37(1), 13–24.
- [7] Afzal, M. J., Javaid, F., Tayyaba, S., Ashraf, M. W., & Hossain, M. K. (2020). Study on the induced voltage in piezoelectric smart material (PZT) using ANSYS electric & fuzzy logic.
- [8] Afzal, M. J. (2020). Study of constricted blood vessels through ANSYS fluent. *Blood vessels*, 27, 11-2020.
- [9] Sharafian, A., & Bahrami, M. (2014). Assessment of adsorber bed designs in waste-heat driven adsorption cooling systems for vehicle air conditioning and refrigeration. *Renewable and Sustainable Energy Reviews*, 30, 440-451.
- [10] Tran, M. K., Mevawalla, A., Aziz, A., Panchal, S., Xie, Y., & Fowler, M. (2022). A review of lithium-ion battery thermal runaway modeling and diagnosis approaches. *Processes*, 10(6), 1192.

Presenter Biography



Rodrigo Amorim Dias is an R&D Engineer at Motul, specializing in dielectric fluids for thermal management of batteries and electronic systems. He holds an Engineer's degree in Chemical Process Engineering from INSA Rouen (2017), and an Engineer's degree in Energy and Products from IFP School (2019). He applies his expertise in thermal management and innovation to develop high-performance lubrication and cooling solutions.